International Journal of Research in Agronomy

SK Tiwari
Department of ITE&C, Andhra Pradesh Space Applications Centre (APSAC), Government of Andhra Pradesh, Vijayawada, Andhra Pradesh, India

V Raghu
Department of ITE&C, Andhra Pradesh Space Applications Centre (APSAC), Government of Andhra Pradesh, Vijayawada, Andhra Pradesh, India

Identification of optimal hyperspectral wavelength to discriminate maize and sorghum crops using AVIRIS-NG data in Guntur district, Andhra Pradesh, India

SK Tiwari and V Raghu

Abstract
In this study, we utilized AVIRIS-NG hyperspectral data captured during the Rabi season in February 2018 in a region of Guntur District, Andhra Pradesh, where Maize and Sorghum crops are extensively cultivated. Despite having parallel crop calendars and spectral similarities, distinguishing between Maize and Sorghum crops during similar vegetative growth stages poses a challenge. The high spectral resolution of AVIRIS-NG data allows for precise identification of subtle changes in the objects under study.
The key finding of our research is the identification of sensitive spectral bands within specific wavelength regions that facilitate the differentiation of these two visually similar crops. Our results indicate that the spectral range from 1553 nm to 1749 nm of AVIRIS-NG data provides optimal discrimination between Sorghum and Maize crops, irrespective of their growth stages. Notably, the wavelengths at 1649 nm and 1654 nm emerge as particularly suitable for distinguishing between Maize and Sorghum crops, as indicated by statistical separability measures such as Wilks' Lambda and F-Value. At these wavelengths, we observed significant results with Wilks' Lambda values of 0.388 and 0.387, and F-Values of 39.29 and 39.46, respectively, further supporting their efficacy in crop discrimination.

Keywords: AVIRIS-NG, hyperspectral, maize, sorghum, spectral bands

Introduction

Hyperspectral data offers significant advantages over traditional multi-spectral data by providing detailed information across the electromagnetic spectrum. Hyperspectral sensors, which are passive sensors, capture hundreds of narrow bands simultaneously, organizing them into what is termed a hyperspectral data cube (Schweizer and Jose, 2001) [9]. This technology provides spectroscopic data across narrow, contiguous spectral bands spanning the visible, near-infrared, and short-wave infrared regions of the electromagnetic spectrum (Hong *et al*., 2002) [6]. The narrow and contiguous bands enable precise detection of absorption features, a capability not achievable with multi-spectral sensors, facilitating accurate vegetation identification and estimation of biochemical content.
Goetz *et al*. (1985) [5] demonstrated in their study the ability to detect and quantify various earth resource materials using hyperspectral remote sensing data, whether collected from airborne or space-borne platforms. Furthermore, hyperspectral imagery has proven effective for quantitative classification and characterization of crops and vegetation properties (Richard Beck, 2003) [8]. Recent advancements in hyperspectral sensor technology, such as the Airborne Visible Infrared Imagine Spectrometer-Next Generation (AVIRIS-NG), have further enhanced capabilities. AVIRIS-NG is an airborne hyperspectral sensor that captures data in the wavelength range from 380 nm to 2510 nm, boasting high spatial resolution (5m) and high spectral resolution (5 nm).
Recent studies have underscored the utility of hyperspectral remote sensing for various applications beyond crop discrimination. Ben-Dor *et al*. (2002) [2] and Tiwari *et al*. (2015) [12] utilized hyperspectral images for mapping several soil properties, showcasing its effectiveness in soil characterization. Additionally, hyperspectral data has been instrumental in crop stage identification, as demonstrated by Senthilnath *et al*. (2011) [10], indicating its potential for crop monitoring and management.

Corresponding Author:
SK Tiwari
Department of ITE&C, Andhra Pradesh Space Applications Centre (APSAC), Government of Andhra Pradesh, Vijayawada, Andhra Pradesh, India

Furthermore, Schweizer and Jose (2001) [9] highlighted the importance of hyperspectral sensors in capturing detailed spectral signatures, enabling accurate identification and classification of vegetation types. Hong *et al*. (2002) [6] emphasized the advantage of hyperspectral sensors in providing spectroscopic information across narrow contiguous bands, facilitating the detection of subtle variations in vegetation properties.

Richard Beck (2003) [8] provided insights into the quantitative classification and identification of crops and vegetation characteristics using hyperspectral imagery, indicating its versatility in agricultural applications. These findings collectively underscore the potential of hyperspectral remote sensing technology for various enviro nmental monitoring and agricultural management tasks.

Recent literature has continued to explore the applications and advancements of hyperspectral remote sensing. For instance, Yang *et al*. (2020) [16] investigated the use of hyperspectral data for monitoring crop water stress, demonstrating its efficacy in detecting subtle changes in plant physiological status. Additionally, Li *et al*. (2021) [17] explored the potential of hyperspectral imaging for assessing crop nitrogen status, highlighting its utility in precision agriculture practices.

Moreover, advancements in machine learning algorithms have further enhanced the analysis of hyperspectral data. Hu *et al*. (2019) [18] developed a deep learning-based approach for crop classification using hyperspectral imagery, achieving high accuracy in distinguishing between different crop types. These recent studies highlight the continued relevance and importance of hyperspectral remote sensing in agricultural monitoring and management.

Building upon this body of literature, our study focuses on leveraging the capabilities of AVIRIS-NG hyperspectral data to identify specific spectral bands capable of discriminating between Maize and Sorghum crops, despite their physiological similarities. By pinpointing these optimal wavelengths, we aim to contribute to the development of more effective remote sensing methodologies for agricultural monitoring and management.

Study area
The study area encompasses the villages of Chinnapalem, Vallabhapuram, Perakalapudi, and Emani within the Duggirala mandal of Guntur District, Andhra Pradesh, India. Geospatially, this region spans from 80° 36' 28.48" E, 16° 24' 21.68" N to 80° 43' 28.36" E, 16° 19' 21.94" N. Maize and Sorghum are the predominant crops cultivated during the Rabi season in this fertile area, which is well-served by a canal command system for irrigation. The geographical distribution of the study area is depicted in Figure 1.
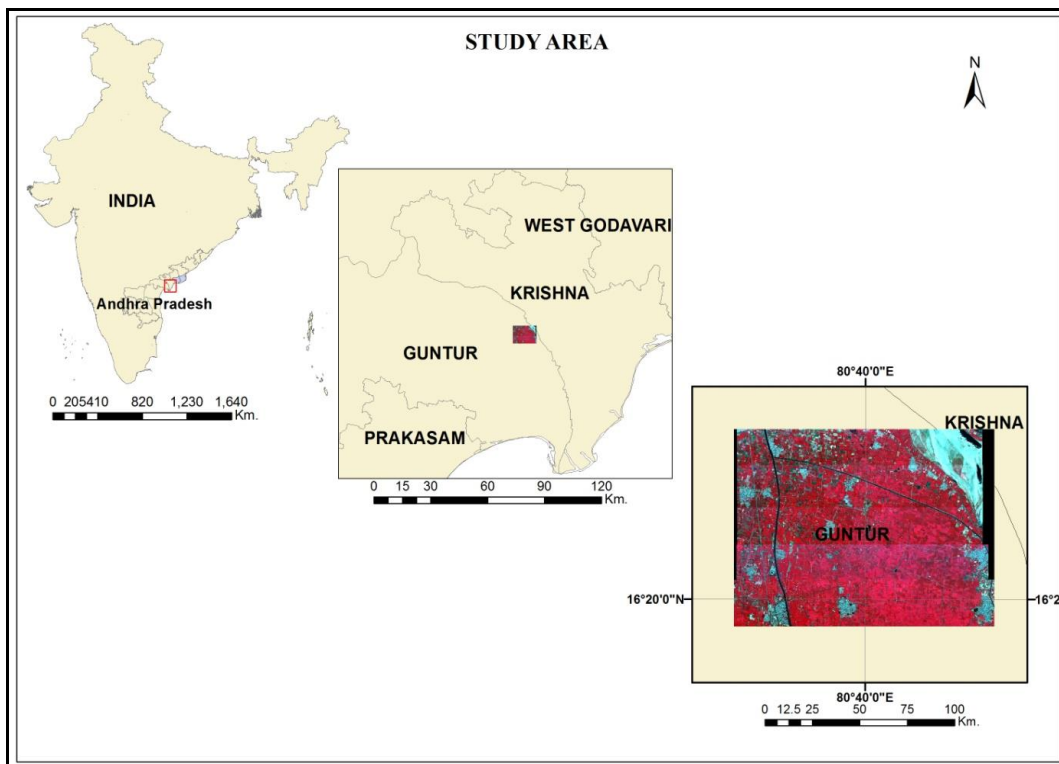
Fig 1: Study Area showing part of Duggirala mandal, Guntur District, Andhra Pradesh

Methodology
1. Data Acquisition
- AVIRIS-NG (Airborne Visible-Infrared Imagine Spectroscopy- Next Generation) data was obtained from the VEDAS portal (https://vedas.sac.gov.in/aviris), developed by the Space Application Centre, ISRO, Ahmedabad. This data is provided under the "Announcement of Opportunity" (AO) for scientific studies.
- Level-2 (reflectance) AVIRIS-NG hyperspectral data processed by NASA was downloaded for the study from the VEDAS portal.

2. Data Rectification
- To address inaccuracies in ground location caused by topographic relief and geometric errors, IRS P6 LISS-IV (5.8m) ortho-rectified satellite data from March 28, 2018, was acquired from the NRSC Data Centre (NDC), NRSC-ISRO.
- Image-to-image rectification was performed using image processing software to rectify the AVIRIS-NG data strips. The rectified strips were then mosaiced to create a synoptic view of the study area.

3. Ground Truth Data Collection

- Ground truth data, including the latitude, longitude, and crop growth stage of maize and sorghum crops, was collected during field visits conducted on February 25th and 26th, 2018.
- The study area predominantly featured maize and sorghum crops, with three main growth stages identified for both crops: vegetative growth, grain filling, and maturity.

4. Spectral Signature Extraction

- Spectral signatures of maize and sorghum crops were extracted using GPS location data, and a spectral library was compiled for all three growth stages of both crops.
- Spectral signatures were plotted to identify the optimal wavelengths/bands for differentiating between maize and sorghum crops, regardless of growth stage.

5. Statistical Discrimination Analysis

- To strengthen the results, a statistical discrimination analysis was performed using Minitab Statistical Software.
- Multivariate separability measures, including Wilks' Lambda and F-Value, were employed to analyze different wavelengths in the AVIRIS-NG spectral data of maize and sorghum crops.
- Wilks' Lambda is interpreted as the proportion of variance in the results not explained by an effect. It is commonly used in multivariate analysis of variance (MANOVA) to test for differences between group means on a combination of dependent variables.

$$\Lambda = (|E|)/(|H + E|) \tag{1}$$

where H is the matrix of squares and products of the fitted response and E is the corresponding matrix for the residuals.

$$H = \sum_{j=1}^{m} n_j (\overline{X}_j - \overline{X}_T)(\overline{X}_j - \overline{X}_T)^T \tag{2}$$

Calculate the intergroup cross product matrix H (the variations across groups):

$$E = \sum_{j=1}^{m} \cdot \sum_{i=1}^{n_j} (X_{ij} - \overline{X}_j)(X_{ij} - \overline{X}_j)^T \tag{3}$$

Calculate the residual matrix E (the variations within groups)

Results

AVIRIS-NG data (26th February 2018) is rectified using ortho-rectified IRS P6 LISS-IV sensor data of 28th March 2018. Image to image rectification process is performed to geo-locate the AVIRIS-NG data concerning earth scenario. Five strips of the study area are rectified. After rectification, all the strips are mosaiced.

The collected ground truth data is overlaid on rectified and mosaiced strips of AVIRIS-NG data (Fig-2). The GT data is collected on 25th and 26th February 2018. The study area is mostly covered with Maize and Sorghum crop. The three stages of both the crops are identified. For maize crop the stages identified in the field are; Vegetative growth, Tasseling stage and Maturity stage. For sorghum crop also three growth stages are identified, which are vegetative growth, grain filling and maturity stage. Majority of maize crop is in tasseling stage, and the sorghum crop is in grain filling stage. Other two stages (Vegetative growth and Maturity stage) are identified on marginal scale in the study area. Total 80 observations are collected from the study area.
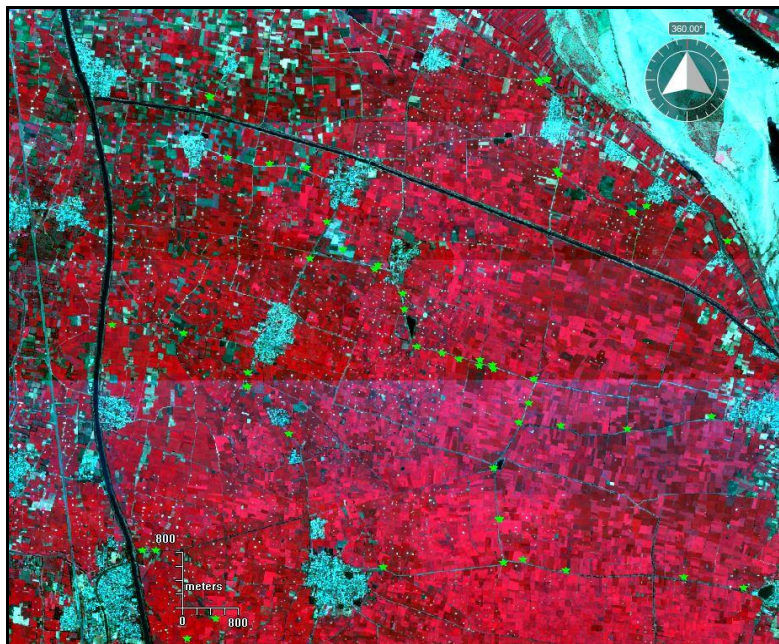
Fig 2: Distribution of ground truth data over on AVIRIS-NG data

The spectral signatures of Maize crop are generated from AVIRIS-NG data using geo-locations collected during field observations. The spectral signature of three stages (vegetative growth, tasseling and maturity stage) are generated and saved as spectral library. The spectral signature of three stages with ground photos are shown in Fig-3. The same steps are followed to generate spectral signature of all three stages of sorghum crop and saved as spectral library. The spectral signature of three stages of sorghum crop with ground photos are shown in Fig-4.
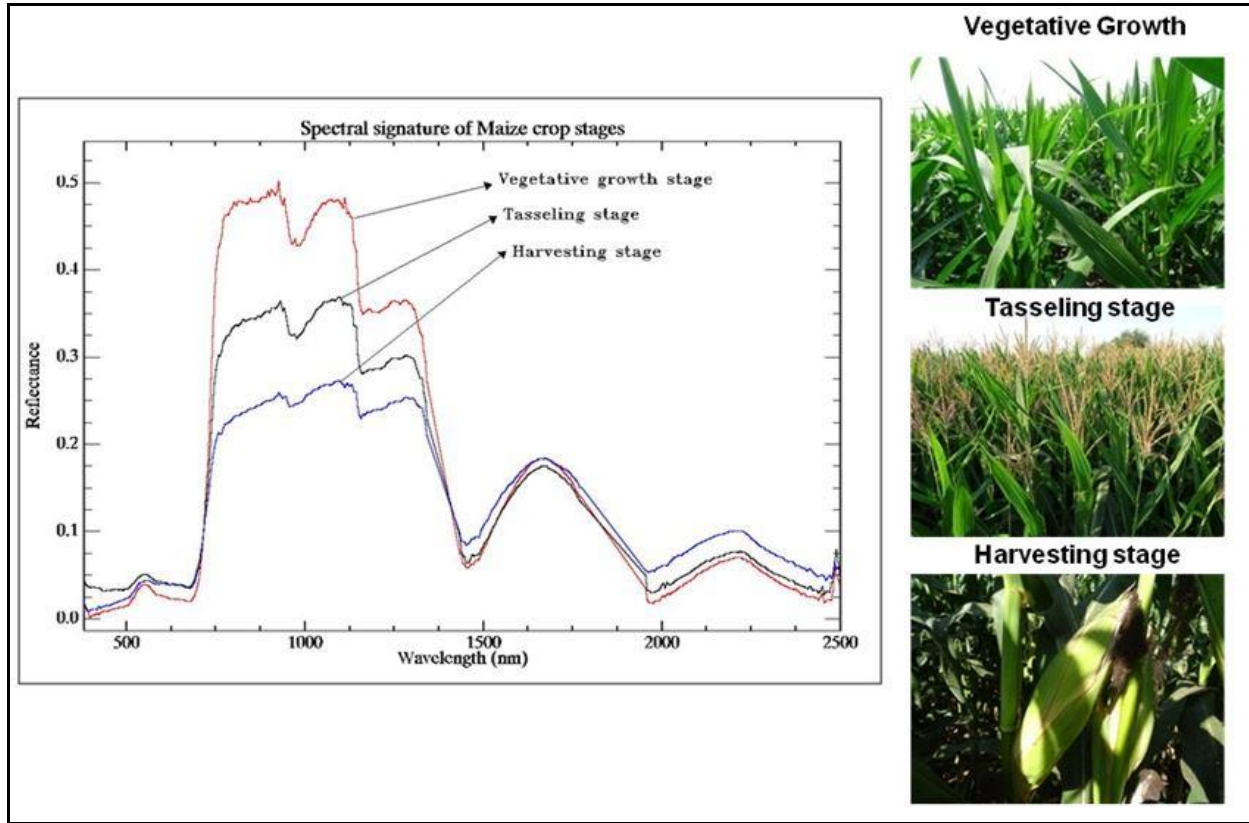
Fig 3: Spectral signature of Maize crop (growth stage wise)
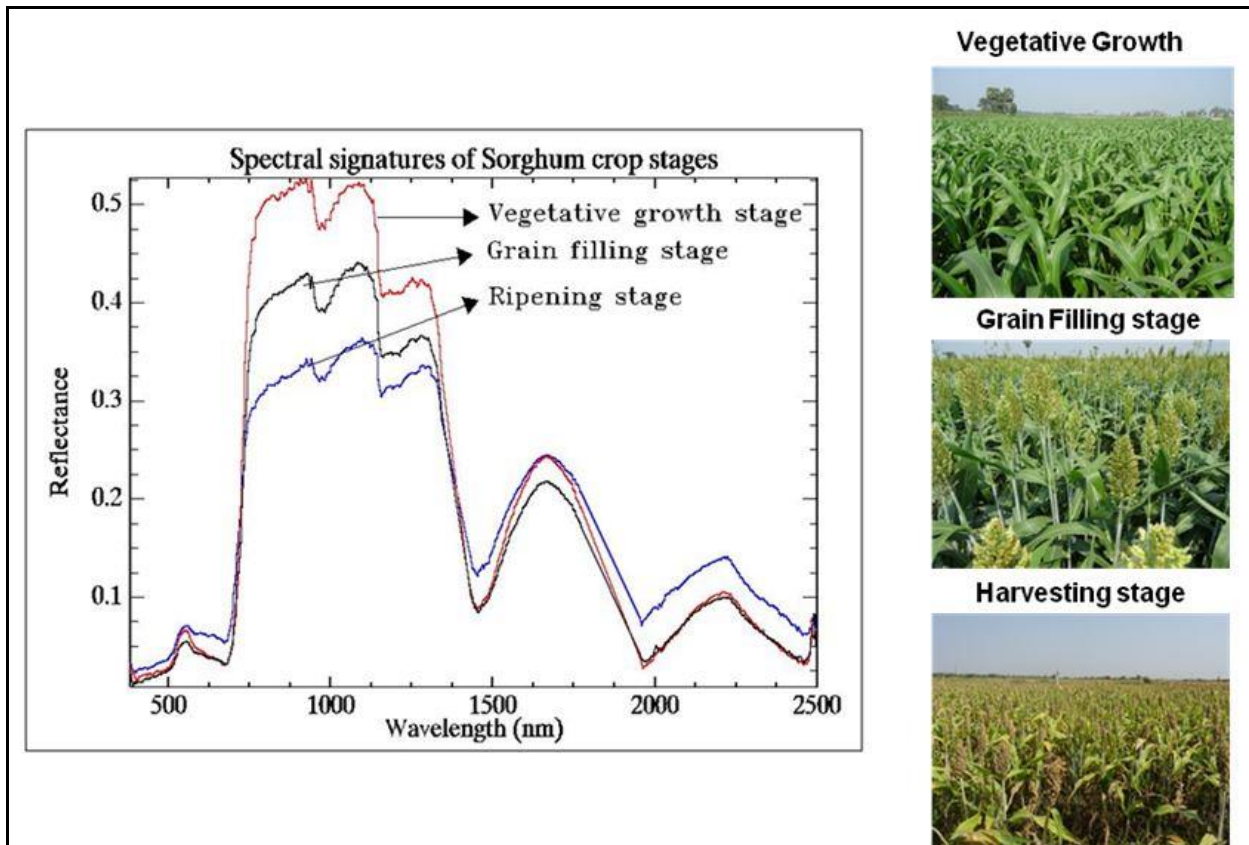
Fig 4: Spectral signature of Sorghum crop (growth stage wise)

During independent growth stages, Maize and Sorghum crops exhibit distinguishable spectral signatures within the 750 nm to 1300 nm spectral range as captured by AVIRIS-NG data. However, when both crops are in similar growth stages simultaneously, identifying or separating their signatures within this range becomes challenging. Consequently, it has been noted that distinguishing between Maize and Sorghum crops is feasible in the spectral range of 1500 nm to 1750 nm, regardless of their growth stages (see Fig-5).
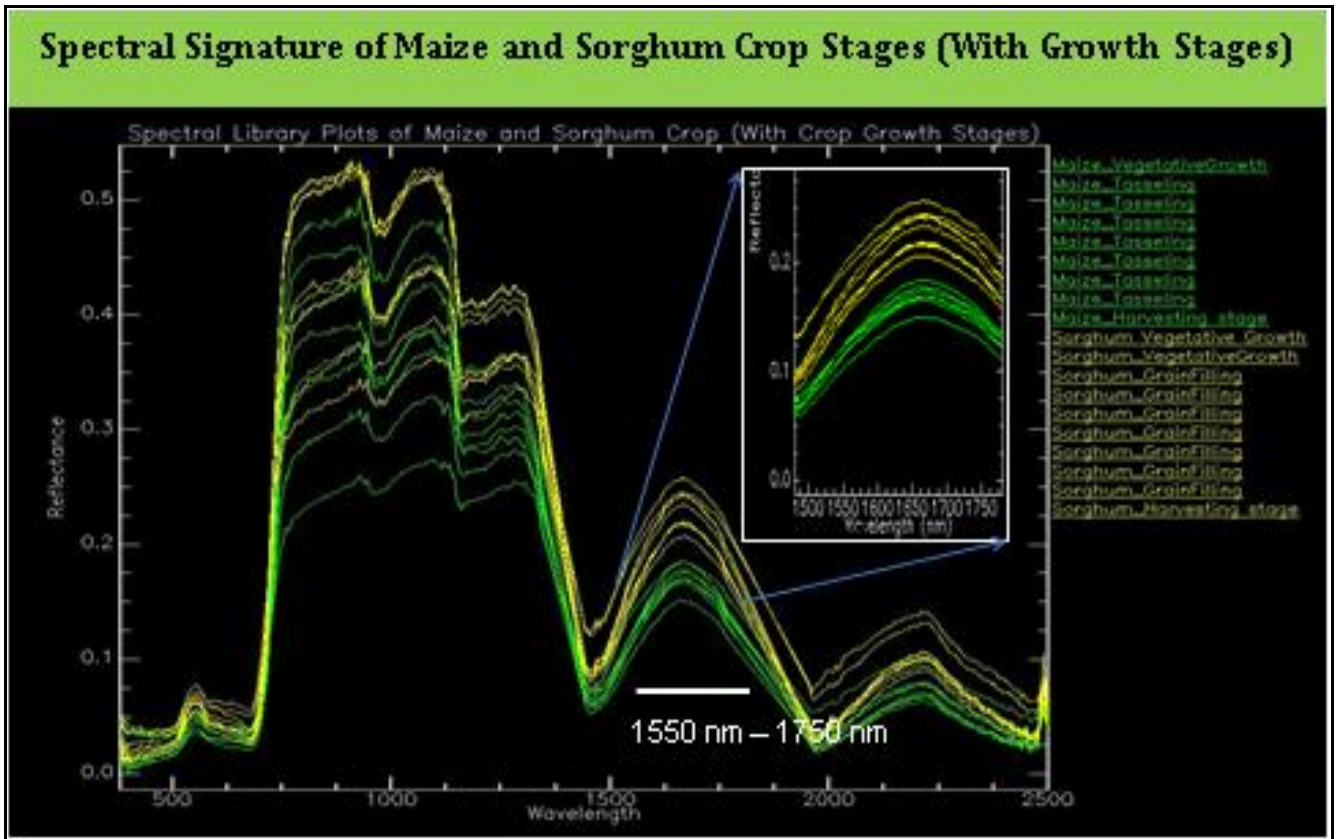
Fig 5: Spectral signature of Maize and Sorghum crop, differentiated in the range of 1500 nm to 1750 nm

Six samples were extracted from various locations across the spectrum to analyze the reflectance values of Sorghum and Maize crops, showcasing the mixing, partial mixing, and non-mixing wavelength bands (see Fig-6). To determine the highest separability between the crops, Wilks' Lambda and F-values were estimated at different wavelengths. Stratified random wavelength locations covering the entire spectrum of AVIRIS-NG, including Visible, Near-Infrared (NIR), and Shortwave Infrared (SWIR) wavelengths, were identified for analysis.

Fig 6: Samples from spectrum showing the mixing of Maize and Sorghum crops

Results revealed Wilks' Lambda values of 0.45, 0.65, 0.82, 0.59, 0.39, and 0.59 at wavelengths 542 nm, 602 nm, 857 nm, 1228 nm, 1654 nm, and 2215 nm, respectively. Corresponding F-Values were observed at the same wavelengths as 30.64, 13.38, 5.56, 17.74, 39.46, and 17.52, respectively. Notably, the lowest Wilks' Lambda value and the highest F-Value were observed at the wavelength of 1654 nm (see Fig-7).

These findings suggest that the wavelength of 1654 nm exhibits the greatest discriminative power between Sorghum and Maize crops, as indicated by the lowest Wilks' Lambda value and the highest F-Value. This wavelength demonstrates significant potential for accurate differentiation between the two crops, contributing valuable insights for further spectral analysis and crop discrimination efforts.

The same criteria were applied to 45 bands within the wavelength range of 1553 nm to 1749 nm, based on the visual separation observed in the reflectance of maize and sorghum crops, as indicated in Figure 5. Within this wavelength region, Wilks' Lambda ranged from 0.39 to 0.82, and F-values ranged from 5.56 to 39.46, as depicted in Figure 7.

Among the wavelengths spanning from 1553 nm to 1749 nm, it was observed that at 1649 nm and 1654 nm, there were significant differences in Wilks' Lambda and F-values. These wavelengths were identified as the most suitable for separating maize and sorghum crops, as evidenced by the statistical separability measures. Wilks' Lambda showed significant results of 0.388 and 0.387, while F-Values were 39.29 and 39.46 at 1649 nm and 1654 nm, respectively.

These findings highlight the efficacy of 1649 nm and 1654 nm wavelengths in effectively distinguishing between maize and sorghum crops, underscoring their importance in spectral analysis and crop discrimination efforts.
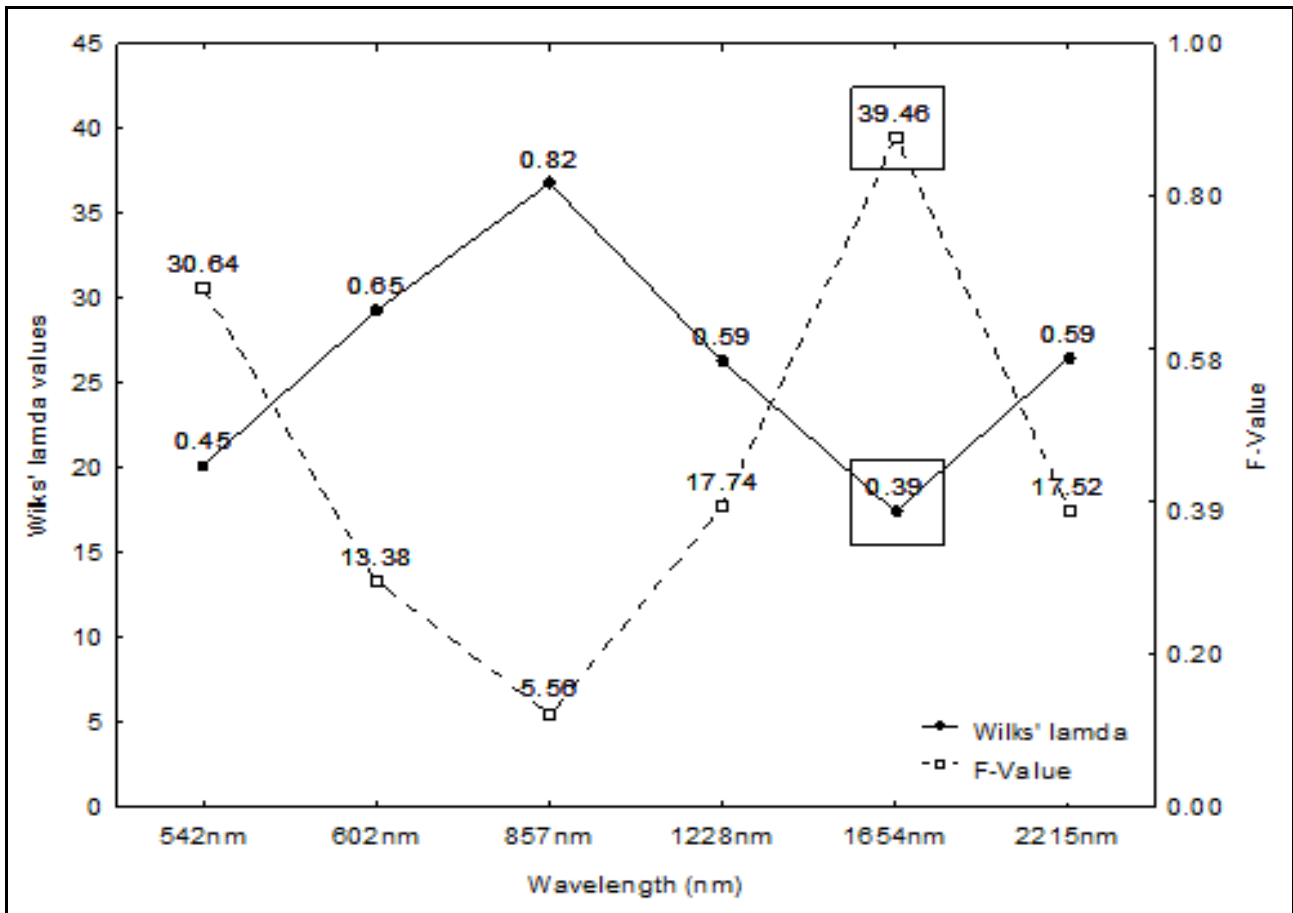
Fig 7: Wilks' lamda and F-Value at 542 nm, 602 nm, 857 nm, 1228 nm, 1654 nm and 2215 nm
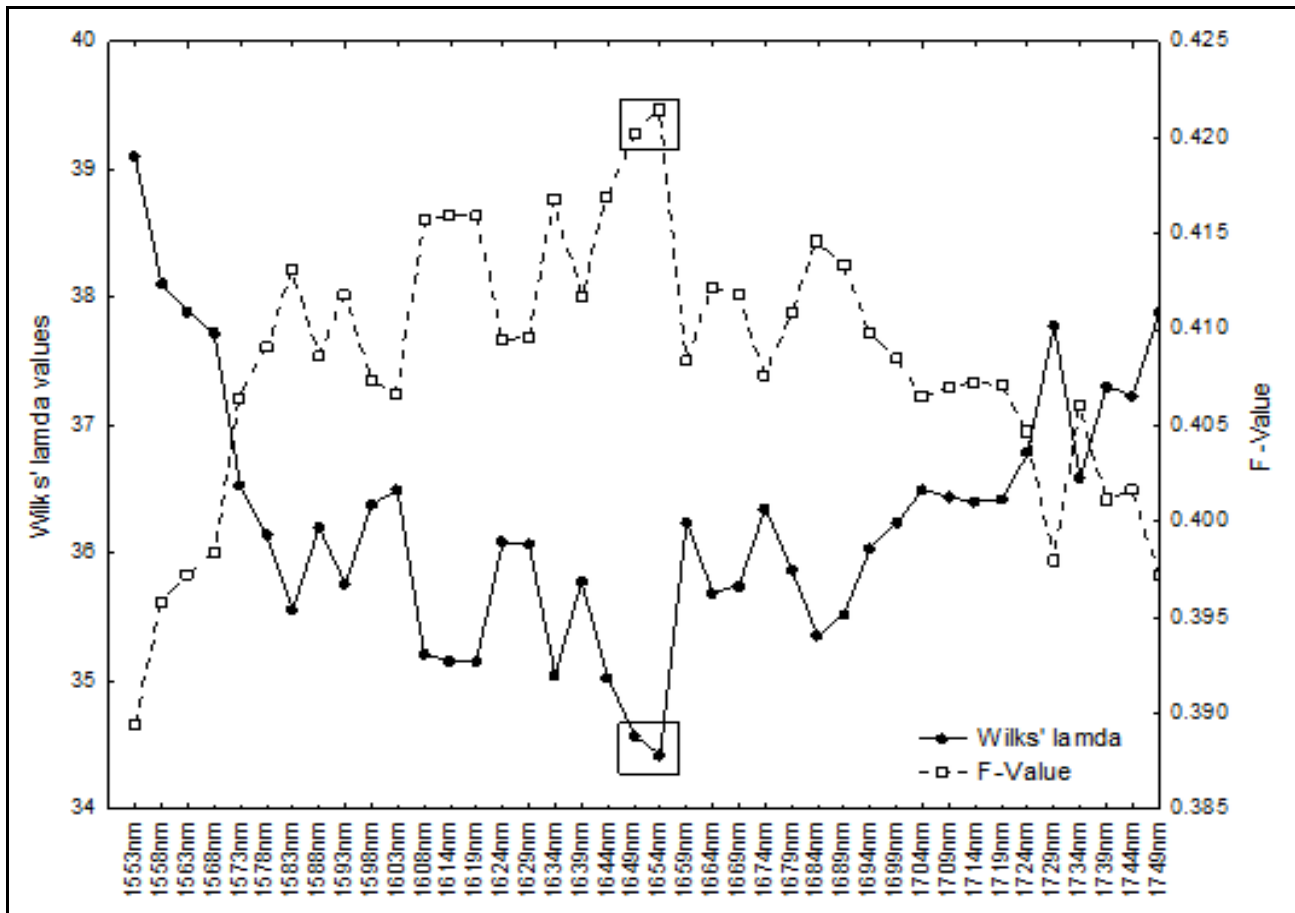
Fig 7: Low Wilks' lamda value and high F-value at 1649 nm and 1654 nm among 1553 nm to1749 nm wavelengths.

Discussion
In this study, AVIRIS-NG reflectance data at Level-2 with 5m spatial resolution underwent preprocessing by NASA to correct fundamental geometric and radiometric errors resulting from vehicle motion during collection. Additional corrections were necessary to address errors due to atmospheric effects such as absorption and scattering, as well as geometric errors related to the topography of the study area. Co-registration of hyperspectral images, as suggested by Brook and Ben-Dor (2011) [3], was deemed significant to ensure accurate spectral analysis. Image rectification with precise ground location matching was conducted using a reference image from IRS P6 LISS-IV, with a similar resolution.

Observations during the study revealed the ability to identify crop growth stages using AVIRIS-NG data. Previous studies, such as Senthilnath *et al*. (2013) [11], have also successfully classified crop stages using hyperspectral data. Spectral signatures within the range of 700 nm to 1300 nm easily distinguish growth stages, leading to mixing of growth stage signatures of both maize and sorghum crops within this range.

Upon plotting the spectra of all growth stages for both crops, it was noted that maize and sorghum crop spectral signatures become distinct in the spectral range of 1500 nm to 1750 nm, falling under the Short Wave Infrared (SWIR) range. This range is particularly sensitive to leaf water content (Wang *et al*., 2008) [13], with reflectance affected by leaf temperature and water content. Additionally, studies by Baret *et al*. (1993) [1] and Lobell and Asner (2002) [7] have highlighted the impact of mineral, organic matter-related absorptions, and soil moisture on reflectance in the SWIR spectral domain, influencing vegetation water indices.

To support these findings, statistical discrimination analysis was conducted using Wilks' Lambda, which inversely measures discrimination between samples. Low Wilks' Lambda values, near zero, indicate high discrimination between samples, as observed in the study. This criterion, noted by Chatfield and Collins (1986) [19], aided in identifying the most suitable bands for discriminating between maize and sorghum crops. Additionally, coupling Wilks' Lambda with F-values strengthened the criteria for band selection. Lower Wilks' Lambda values coupled with high F-values enhanced the identification of the most suitable bands, a criterion also utilized by Manjunath *et al*. (2011) in discriminating spectrally close crops using ground-based hyperspectral data.

Conclusion
The identification of crops that are phenologically similar to each other poses a significant challenge for traditional multi-spectral sensor data. However, our study demonstrates that AVIRIS-NG hyperspectral data has the capability to distinguish between Sorghum and Maize crops, even when they are at similar growth stages. Specifically, our analysis reveals that within the spectral range of 1553 nm to 1749 nm, both crops can be effectively differentiated. Furthermore, the wavelengths of 1649 nm and 1654 nm emerge as the most suitable for distinguishing between Maize and Sorghum crops. This conclusion is supported by significant results obtained from statistical separability measures, including Wilks' Lambda and F-Value, at these specific wavelengths.

The ability to differentiate between these crops using AVIRIS-NG data, particularly at the identified wavelengths, holds great potential for practical applications such as crop identification and yield estimation. By leveraging hyperspectral technology, agricultural monitoring and management efforts can be

significantly enhanced, enabling more accurate assessments of crop health, productivity, and overall agricultural performance. Thus, our findings underscore the importance of hyperspectral remote sensing in addressing the challenges associated with crop identification and management, ultimately contributing to improved agricultural practices and food security.

References
1. Baret F, Jacquemond S, Hanocq JF. The soil line concept in remote sensing. Remote Sensing of Enviro nment. 1993;7:65-82.
2. Ben-Dor E, Patkin K, Abanin, Karnieli A. Mapping of several soil properties using DAIS-7915 Hyperspectral scanner data - a case study over clayey soils in Israel. International Journal of Remote Sensing. 2002;23(6):1043-1062.
3. Brook A, Ben-Dor E. Advantages of the boresight effect in hyperspectral data analysis. Remote Sensing. 2011;3(3):484-502.
4. Gao BC. NDWI—a normalized difference water index for remote sensing of vegetation liquid water from space. Remote Sensing of Environment. 1996;58:257-266.
5. Goetz AF, Vane G, Solomon JE, Rock BN. Imaging spectrometry for earth remote sensing. Science. 1985;228(4704):1147-1153.
6. Hong SY, Sudduth KA, Kitchen NR, Drummond ST, Palm HL, Wiebold WJ. Estimating within field variations in soil properties from airborne Hyperspectral images. ISPRS Commission I/FIOEOS 2002 Conference Proceedings. 2002.
7. Lobell DB, Asner GP. Moisture effects on soil reflectance. Soil Science Society of America Journal. 2002;66:722-727.
8. Richard Beck, "EO-1 User Guide, V.2.3", [http:// eo1.usgs.gov & http://eo1.gsfs.nasa.gov](http://eo1.usgs.gov & http://eo1.gsfs.nasa.gov). 2003.
9. Schweizer S, Jose M. Efficient detection in hyperspectral imagery. IEEE transactions on image processing: a publication of the IEEE Signal Processing Society. 2001;10:584-97.
10. Senthilnath J, Omkar SN, Mani V, Karnwal N. Hierarchical artificial immune system for crop stage classification. Proc. IEEE INDICON. 2011:1-4.
11. Senthilnath J, Omkar SN, Mani V, Karnwal N, Shreyas PB. Crop Stage Classification of Hyperspectral Data Using Unsupervised Techniques. IEEE Journal of Selected Topics in Applied Earth Observations and Remote Sensing. 2013;6(2):861-866.
12. Tiwari SK, Saha S, Kumar S. Prediction Modelling and Mapping of Soil Carbon Content Using Artificial Neural Network, Hyperspectral Satellite Data and Field Spectroscopy. Advances in Remote Sensing. 2015;4:63-72. doi: 10.4236/ars.2015.41006.
13. Wang L, John J, Qu J, Xianjun Hao, Qingping Zhu. Sensitivity studies of the moisture effects on MODIS SWIR reflectance and vegetation water indices. International Journal of Remote Sensing. 2008;29(24):7065-7075.
14. Everitt BS, Dunn G. Applied Multivariate Data Analysis. Edward Arnold. London; c1991. p. 219-220.
15. Polit DF. Data Analysis and Statistics for Nursing Research. Appleton and Lange, Stamford, Connecticut; c1996. p. 320-321.
16. Zhao S, Lin Q, Ran J, Musa SS, Yang G, Yang L, et al, Wang MH. Preliminary estimation of the basic reproduction number of novel coronavirus (2019-nCoV) in China, from 2019 to 2020: A data-driven analysis in the early phase of the outbreak. International journal of infectious diseases. 2020 Mar 1;92:214-217.
17. Shen X, Tang H, McDanal C, Wagh K, Fischer W, Li D, et al. SARS-CoV-2 variant B. 1.1. 7 is susceptible to neutralizing antibodies elicited by ancestral spike vaccines. Cell host & microbe. 2021 Apr 14;29(4):529-539.
18. Wang J, Chen Y, Hao S, Peng X, Hu L. Deep learning for sensor-based activity recognition: A survey. Pattern recognition letters. 2019 Mar 1;119:3-11.
19. Chatfield C. Introduction to multivariate analysis. Routledge; c2018 Feb 19.
20. Nataraj L, Karthikeyan S, Jacob G, Manjunath BS. Malware images: visualization and automatic classification. In Proceedings of the 8th international symposium on visualization for cyber security; c2011. p. 1-7.